Photoluminescence of Ga-doped ZnO film grown on c-Al_2O_3 (0001) by plasma-assisted molecular beam epitaxy

H. C. Park and D. Byun
Department of Advanced Materials Engineering, Korea University, Sungbuk Ku, Anam Dong 5-1, Seoul 136-701, Korea

B. Angadi,[a] D. Hee Park, and W. K. Choi[b]
Materials Science and Technology Research Division, Korea Institute of Science and Technology, Cheongryang P.O. Box 131, Seoul 130-650, Korea

J. W. Choi
Thin Film Materials Research center, Korea Institute of Science and Technology, Cheongryang P.O. Box 131, Seoul 130-650, Korea

Y. S. Jung
Department of Materials Science and Engineering, MIT, 77 Massachusetts Avenue, Cambridge, Massachusetts 02139, USA

(Received 22 June 2007; accepted 31 July 2007; published online 12 October 2007)

High quality gallium doped ZnO (Ga:ZnO) thin films were grown on c-Al_2O_3(1000) by plasma-assisted molecular beam epitaxy, and Ga concentration N_{Ga} was controlled in the range of $1\times10^{18}-2.5\times10^{20}/cm^3$ by adjusting/changing the Ga cell temperature. From the low-temperature photoluminescence at 10 K, the donor bound exciton I_8 related to Ga impurity was clearly observed and confirmed by comparing the calculated activation energy of 16.8 meV of the emission peak intensity with the known localization energy, 16.1 meV. Observed asymmetric broadening with a long tail on the lower energy side in the photoluminescence (PL) emission line shape could be fitted by the Stark effect and the compensation ratio was approximately 14–17% at $N_{Ga}\geqslant 1\times10^{20}/cm^3$. The measured broadening of photoluminescence PL emission is in good agreement with the total thermal broadening and potential fluctuations caused by random distribution of impurity at N_{Ga} lower than the Mott critical density. © *2007 American Institute of Physics*.
[DOI: 10.1063/1.2783956]

I. INTRODUCTION

Since recently, ZnO has emerged as a new candidate for ultraviolet (UV)-blue light emitting diodes/laser diodes (LEDs/LDs), replacing III-V compound semiconductors, due to its large band gap of 3.37 eV, high exciton binding energy of 60 meV, and higher optical gain ($300\ cm^{-1}$) than that of GaN ($100\ cm^{-1}$).[1–4] Also, excitonic UV emission at 375 nm from ZnO at room temperature implies a better excitation efficiency of phosphor for solid state lighting compared to that of GaN at 405 nm. In addition, availability of 2 in. ZnO single crystal makes ZnO the most promising for the realization of high efficient ZnO-based homojunction devices. Efforts have been made continuously for developing high quality ZnO employing various techniques to realize high performance electro-optic devices. In addition to developing high quality intrinsic ZnO epilayer, it is necessary to produce high quality heavily doped n-type ZnO for achieving high efficiency LED and LD. Ga has a nearer ionic radius (0.62 Å) and covalent radius (1.26 Å) to Zn (0.74 Å, 1.31 Å) compared to In (0.81 Å, 1.44 Å) and Al (0.5 Å, 1.26 Å). Ga–O covalent bonding length (1.91 Å) is much closer to that of Zn–O (1.97 Å) than In–O (2.1 Å) and Al–O (2.7 Å), therefore Ga doping has been proposed to have superior advantages over other group III n-type dopants.[5] Besides, Ga doped ZnO showed a strong near-band-edge (NBE) emission even at room temperature (RT) and lower oxidation rate of Ga source during growth. These advantages have stimulated ZnO researchers to develop and analyze epitaxial ZnO:Ga films. However, in-depth knowledge and scrutiny on the optical properties of ZnO:Ga on realizing and predicting the performances of ZnO-based optoelectronic devices are still deficient.

In this study, the low-temperature photoluminescence (PL) properties of heavily doped ZnO:Ga ($1\times10^{18}-2.5\times10^{20}\ cm^{-3}$) are explored and discussed in terms of charge fluctuation and impurity band conduction.

II. EXPERIMENT

The ZnO films were deposited on α-Al_2O_3(0001) single crystals by plasma-assisted molecular beam epitaxy (PA-MBE). An elemental Knudsen cell was used to supply zinc atoms of 6N purity, and the temperature of the cell was maintained at 355 °C during deposition. In order to control the n-type doping concentration, Ga cell temperature was varied from 450 to 650 °C. Active oxygen species was generated and spread over the sapphire substrate through a radio-frequency plasma source activated at the power of 450 W.

[a]Present address: Department of Physics, Bangalore University, Bangalore 560 056, India. Electronic mail: brangadi@gmail.com
[b]Author to whom correspondence should be addressed. Electronic mail: wkchoi@kist.re.kr

 © 2007 American Institute of Physics

Downloaded 16 May 2011 to 143.248.111.110. Redistribution subject to AIP license or copyright; see http://jap.aip.org/about/rights_and_permissions

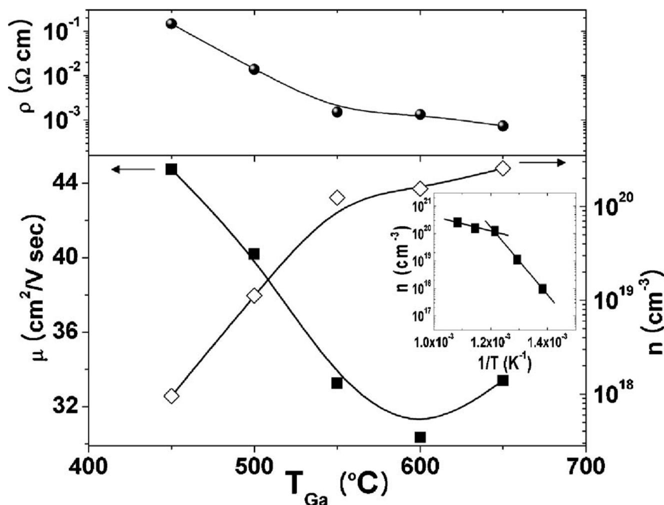

FIG. 1. Measured mobility and resistivity of Ga:ZnO. Inset shows the change of Ga concentration as a function of $1/T$.

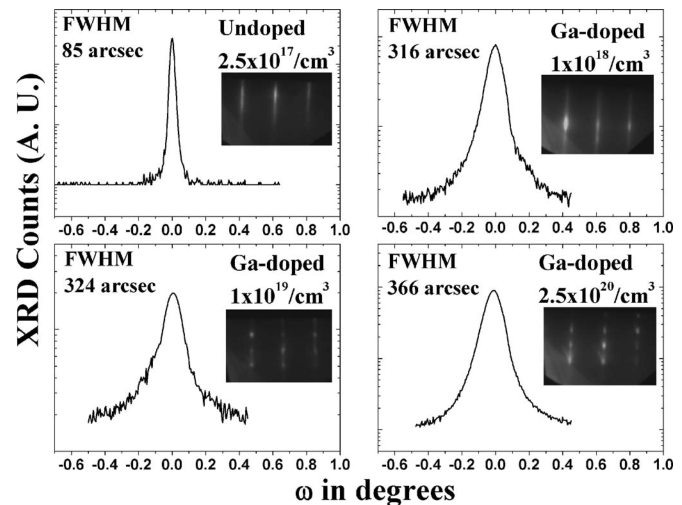

FIG. 2. X-ray ω-rocking curves (XRC) and RHEED patterns of undoped ZnO and Ga:ZnO grown on c-Al_2O_3(0001).

Detailed conditions for preparing and cleaning sapphire substrate were reported elsewhere.[6,7] The low-temperature buffer layer with thickness of 15 nm was grown at 500 °C and was thermally treated at 800 °C for 30 min. Then, the growth was restarted at 720 °C and continued for 3 h. The total thickness of the film was about 800 nm. *In situ* RHEED (Oxford Applied Research, LEG 110) patterns were observed to monitor the growth mode and surface status of the films during deposition. The crystalline quality of the deposited films was estimated by XRC (Bruker AXS, D8 Discover). Room temperature Hall measurement was performed by Van der Pauw technique with magnetic field of 0.3 T. Temperature-dependent photoluminescence was carried out with an excitation source of $\lambda = 325$ nm He–Cd laser (25 mW).

III. RESULTS AND DISCUSSIONS

A. Electrical properties of Ga:ZnO

Figure 1 shows the room temperature Hall measurement results. With increasing the Ga cell temperature from 450 to 650 °C, the electron concentration increases from about $1\times10^{18}/\mathrm{cm}^3$ to $2.5\times10^{20}/\mathrm{cm}^3$. The carrier density exponentially increases with Ga cell temperature and is in agreement with the exponential dependence of vapor pressure on the temperature through the Clausius-Clapeyron equation (equilibrium vapor pressure $\sim e^{(-\Delta H/RT)}$). The 4.4 times smaller slope of $\ln(n)$ vs (1/T) graph (inset of Fig. 1) for the higher cell temperature region than that of the lower cell temperature case means the decrease of Ga activation ratio when heavily doped above the carrier density of 10^{20} cm^{-3}. While Ko *et al.* reported that the carrier density of Ga:ZnO is saturated at around $10^{20}/\mathrm{cm}^3$, our results in Fig. 1 show a steady increase of carrier density up to $2.5\times10^{20}/\mathrm{cm}^3$. Because of the augmented ionized impurity scattering as the doping level increases, the Hall mobility decreased from 44.8 to 30.4 cm^2/V s, which is comparable with the 36.7–51.1 cm^2/V s reported.[8]

B. XRD and RHEED

Figure 2 presents the x-ray diffraction (XRD)-rocking curve (XRC) of the ZnO (0002) films with different carrier densities. The inset picture shows the corresponding $\langle 1\bar{2}10\rangle$ reflection high-energy electron diffract (RHEED) patterns. The undoped film has the narrowest full width at half maximum (FWHM) of 85 arc sec. The FWHM of XRC for the symmetric (0002) diffraction implies the presence of tilt component of the in-plane mosaic misorientation (tilt), which is well correlated with the density of screw dislocations.[9] The FWHM abruptly increases to 316 arc sec for the Ga doped film with carrier density of 1×10^{18}, and gradually increases further for heavier doping concentrations. The local strain field induced by the smaller ionic radius of substituted Ga (0.61) than Zn (0.74) and the point defects associated with the Ga are thought to be responsible for the observed line broadening. Because the Ga atoms should be randomly distributed on an atomic scale, where there exist enough Ga ions to reduce the lattice constant, the formation of threading dislocations could be supposed. These FWHM values are significantly higher than 94 arc sec reported by Ko *et al.* who employed thick GaN films (as templates) of much less lattice misfit of 2.2% compared with 18.3% of c-plane sapphire substrates with ZnO.[8] However, the same research group reported 281–350 arc sec when they used sapphire substrates. The undoped ZnO film shows a sharp and streaky RHEED pattern representing two-dimensional growth mode of ZnO. On the other hand, as Ga content increases, the spotty character of RHEED pattern is enhanced. For the MBE system employed in this research, 720 °C was found to be the optimum growth temperature for obtaining two-dimensional growth mode on a low-temperature ZnO homobuffer layer, and it was suggested that the energy of adatoms should be sufficient to increase the surface diffusion for the two-dimensional growth. The adatom mobility of oxygen atoms or ions may be limited by the larger electric field induced by the trivalent Ga ions than that of divalent Zn ions on the growing surface, and consequently, for higher Ga flux, the growth of ZnO:Ga deviates more from two-dimensional growth mode.

Downloaded 16 May 2011 to 143.248.111.110. Redistribution subject to AIP license or copyright; see http://jap.aip.org/about/rights_and_permissions

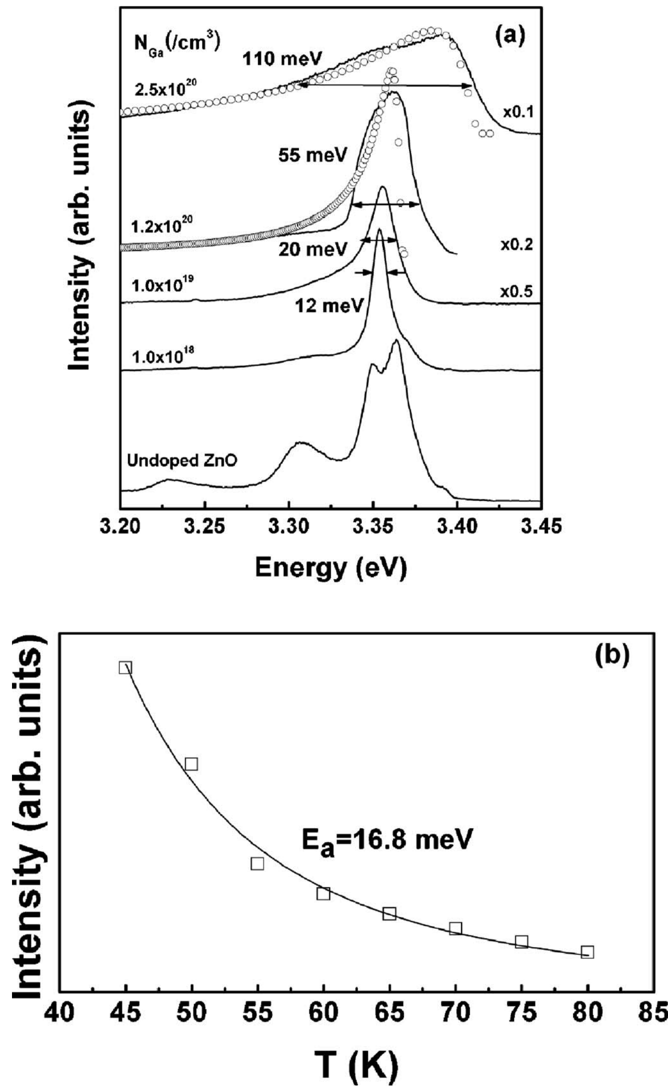

FIG. 3. (a) Photoluminescence spectra (solid curves) of Ga:ZnO taken at 10 K and theoretically calculated fitting curves (open circles) by the Stark effect, and (b) Arrhenius plot of the emission intensity as a function of temperature.

C. PL studies

The PL spectra of undoped and Ga-doped ZnO films measured at 10 K are shown in Fig. 3(a). Two peaks at 3.3636 (I_4) and 3.3491 (I_{11}) are found for the PL spectrum of undoped ZnO. The I_4 line was previously reported to be originated from the recombination of excitons bound to hydrogen,[10,11] while the origin of I_{11} line is still unknown. On the other hand, Ga doping appreciably changes the aspect of the near-band-edge emission. Even the lowest Ga-doping level of $\sim 10^{18}$ cm^{-3} eliminates bound-exciton emission lines observed for the undoped ZnO and generates one dominant peak near the band edge at 3.3554 eV. The temperature dependence of the PL intensity can be expressed by Eq. (1), where C_1 is the fitting parameter and ε_1 is the activation energy.

$$I = I_o/[1 + C_1 \exp(-\varepsilon_1/kT)]. \tag{1}$$

Here, the luminescence intensity I is defined as the area of an emission band and calculated by the Lorentzian distribution.

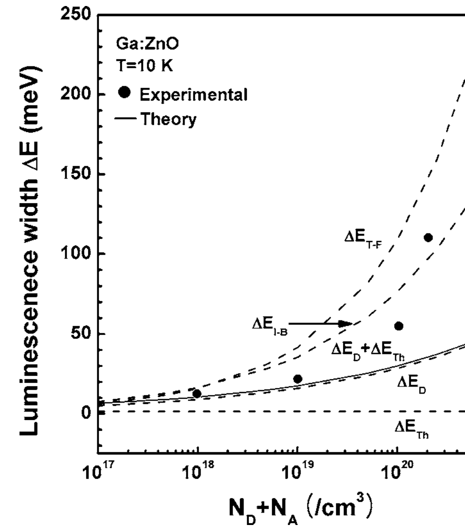

FIG. 4. Experimentally observed linewidth of PL emission (solid circle) and the theoretically calculated one (dotted curves); broadening due to ΔE_{Th} (thermal), and impurity fluctuation in cases of ΔE_D (nondegenerate) or $\Delta E_{\mathrm{T\text{-}F}}$ (degenerate) and $\Delta E_{\mathrm{I\text{-}B}}$ (impurity band).

By fitting the Arrhenius plot of the exciton emission intensity as presented in Fig. 3(b), which corresponds to the energy for thermal release of excitons from the neutral donors, $[D_o, X] \rightarrow D_o + X$, the activation energy for the peak is estimated as 16.8 meV. This value is very close to the reported value of 16.1 meV for the localization energy of exciton bound donor I_8.[11] This has been proposed to originate from the recombination of exciton bound to neutral Ga donor. As the concentration increases, the broadening becomes larger from 12 meV at $n_{\mathrm{Ga}} = 1 \times 10^{18}/\mathrm{cm}^2$ to 110 meV at $n_{\mathrm{Ga}} = 2.5 \times 10^{20}/\mathrm{cm}^3$. Random distribution of Ga dopant leads to potential fluctuation, resulting in the broadening of the luminescent emission lines.[12] In the former studies,[13,14] the potential fluctuations were calculated assuming that their effect is limited by the distance to the screening radius, namely, the Debye or the Thomas–Fermi screening radius for nondegenerate and for degenerate doping concentrations, respectively.

The broadening, i.e., FWHM, of the NBE transition due to doping charge fluctuations is given by[13]

$$\Delta E_{\mathrm{FWHM}} = \frac{2e^2}{3\pi\varepsilon}\sqrt{(N_D + N_A)\frac{\pi r_s}{3}}e^{-(3/4)}2\sqrt{2\ln 2}, \tag{2}$$

where ε is the dielectric constant, N_D (N_A) stands for the concentration of donors (acceptors), and r_s is either the Debye or Thomas-Fermi screening radius. The factor $2\sqrt{2\ln 2}$ accounts for the difference between the standard deviation and the FWHM of a Gaussian distribution.[15] Based on the nondegenerate (Boltzmann) and degenerate statistics (Fermi-Dirac) for an isotropic and parabolic band, the screening radii are, respectively, obtained as Eq. (3).

$$r_D = \sqrt{\varepsilon kT/e^2 n}, \quad r_{\mathrm{TF}} = \pi^{2/3}\sqrt{\frac{\varepsilon\hbar^2}{2^2 m^*(3n)^{1/3}}}. \tag{3}$$

Using Eqs. (2) and (3) the corresponding energy broadenings ΔE_{TF} (Thomas-Fermi) and ΔE_D (Debye) can be obtained. Experimental data and theoretical calculation are compared in Fig. 4. As shown in Fig. 4, at the concentration

Downloaded 16 May 2011 to 143.248.111.110. Redistribution subject to AIP license or copyright; see http://jap.aip.org/about/rights_and_permissions

below $M_{crit}(\approx 7\times 10^{19}/\text{cm}^3)$,[14,16] the measured broadening of PL emission at 10 K is quite in good agreement with the total broadening ΔE_T, which is the sum of two uncorrelated broadening: due to thermal broadening (ΔE_{Th}) and that due to potential fluctuations (ΔE_D) caused by random distribution of dopants, if r_s is assumed as the Debye screening radius, which is similar to the result with the previous Si:GaN.[12] On the other hand, at concentrations higher than N_{crit}, the observed broadening becomes larger than the calculated ΔE_T as the concentration increases. Since the above model is applicable only for $N_D < N_{crit}$, for better understanding of large broadening as the N_{Ga} increases higher than N_{crit}, combined high doping effect such as band-edge energy fluctuation, i.e, band filling, Burstein-Moss shift, and band gap narrowing, should be further considered. As impurity concentration increases, it can be intuitively conjectured that the overlapping impurity state forms impurity band and the Fermi level enters into the conduction band. At low temperatures, carriers can propagate within the impurity band without entering the conduction band, which, in turn, makes the process to be called impurity band conduction instead of hopping conduction. Impurity bandwidth is approximately given by the overlap integral between donors separated by the average distance $N_D^{-1/3}$. The bandwidth is approximately equal to the interaction energy,[12]

$$\Delta E_{\text{I-B}} \approx \frac{e^2}{4\pi\varepsilon N_D^{11/3}}, \tag{4}$$

This impurity bandwidth will be intrinsically related to the impurity band broadening ($\Delta E_{\text{I-B}}$) of the PL emission lines and is plotted in Fig. 4 as a function of N_{Ga}. Besides impurity band formation for high doping, broadening due to random charge fluctuation is calculated using Thomas-Fermi screening radius for this degenerate system and is illustrated in Fig. 4. At $N_{Ga} > N_{crit}$, the experimentally observed broadenings show a tendency to have similar values rather closer to $\Delta E_{\text{I-B}}$ than to $\Delta E_{\text{T-F}}$.

In particular, the asymmetric broadening with a long tail on the lower energy side in the PL emission line shape is observed and the FWHM of the asymmetric line increases. This type of asymmetric broadening in bound-exciton (BX) emission line has been theoretically described in terms of Stark effect caused by charged impurity.[17] Assuming that only the nearest impurity to a BX obeying the Poisson distribution contributes to the Stark effect, the emission intensity I of the BX emission can be expressed, from Eq. (2), as

$$I(E) = \pi[e^4/2\mu\varepsilon_0^{\,2}\varpi^2_{l0}]^{3/4}N_{ci}|\Delta E|^{-7/4}\exp\left[-\frac{4\pi}{3}N_{ci}a_B^{*3}\left(\frac{4E_b}{\Delta E}\right)^{3/4}\right], \tag{5}$$

where N_{ci} is the concentration of charged impurity, a_B^* is the effective Bohr radius (1.4 nm), and E_b (60 meV) is the binding energy of the intrinsic exciton. The maximum of the spectrum lies at the point $\Delta E = -4(4\pi N_{ci}/7)^{4/3}a_o 4E_b$ below the energy of the bound exciton which was affected by screening effect. The simulated curves according to Eq. (5) for the emission lines of the samples having higher concentration than the Mott critical density N_{crit} are illustrated (white circles in Fig. 3.), and the estimated concentrations of charged particles are $N_{ci} = 1.4\times 10^{19}/\text{cm}^3$ and $4.4\times 10^{19}/\text{cm}^3$ for $N_{Ga} = 1\times 10^{20}/\text{cm}^3$ and $2.5\times 10^{20}/\text{cm}^3$, respectively. N_{ci} corresponds to $2N_A$ (N_A: acceptor concentration) at low temperature, and the calculated compensation ratios are $N_{ci}/N_{Ga} = 0.14$ and 0.17, respectively. These values are relatively higher than that ever reported (0.06), but still imply small compensation of carrier up to $2.5\times 10^{20}/\text{cm}^3$. The larger broadening at $N_{Ga} = 2.5\times 10^{20}/\text{cm}^3$ is caused by the fact that higher compensation induces greater fluctuation.

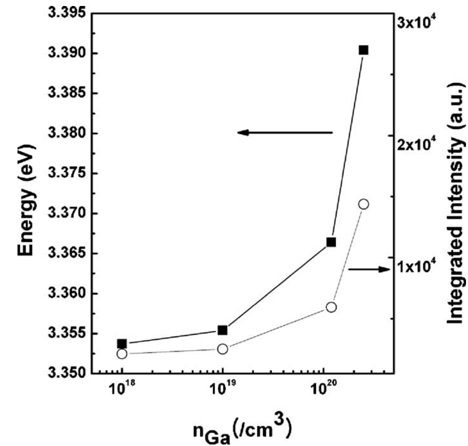

FIG. 5. Variations of energy position and total intensity of the emission peaks.

Figure 5 presents the changes of integrated intensity and the shift of the NBE as a function of Ga concentration. Relatively low intensity at low N_{Ga} can be mainly attributed to the nonradiative transition. However, in general, radiative transition increases with the increment of doping concentration. This monotonous increase in luminescence efficiency up to 7 implies that the defect levels in the Ga–ZnO films do not increase with the increase of N_{Ga} and, thus, the grown Ga-doped ZnO is of high quality. This result is coincident with the cases of Si-doped GaN and Ga-doped ZnO grown by laser MBE.[12,14]

IV. CONCLUSIONS

Through the low-temperature PL for Ga-doped ZnO, Ga-induced donor bound exciton I_8 was clearly observed and confirmed by obtaining the activation energy of 16.8 meV. As the concentration increased, the total area of the intensity increased up to $N_{Ga} = 2.5\times 10^{20}/\text{cm}^3$. Moreover, the asymmetric broadening with a long tail on the lower energy side in the PL emission line shape at 10 K is observed and the FWHM of the asymmetric line increases from 12 to 110 meV, which can be well described by the Stark effect. The broadening of the linewidth coincides with the sum of thermal broadening and impurity fluctuation, assuming that the charge screening effect within the Debye screening radius at N_{Ga} is lower than the Mott crtical density. At higher N_{Ga}, larger broadening can be intuitively explained in terms of impurity band formation and Thomas-Fermi screening radius due to degeneracy.

Downloaded 16 May 2011 to 143.248.111.110. Redistribution subject to AIP license or copyright; see http://jap.aip.org/about/rights_and_permissions

ACKNOWLEDGMENTS

This work is financially supported by both the KIST Future-Resource Program (2E19880) and the KOSEF Program under Contract No. R01-2004-000-10715-09.

[1] D. C. Look, D. C. Reynolds, C. W. Litton, R. L. Jones, D. B. Eason, and G. Cantell, Appl. Phys. Lett. **81**, 1830 (2002).
[2] M. Kawasaki, A. Ohotomo, I. Obkubo, H. Koinuma, Z. K. Tang, P. Yu, G. K. L. Wong, B. P. Zhnag, Y. Segawa, Mater. Sci. Eng., B **B56**, 239 (1998).
[3] Y. F. Chen, H. J. Ko, S. K. Hong, and T. Yao, Appl. Phys. Lett. **76**, 559 (2000).
[4] D. M. Bagnell, Y. F. Chen, Z. Zhu, T. Yao, M. Y. Shen, and T. Goto, Appl. Phys. Lett. **73**, 1038 (1998).
[5] W. B. Pearson, *Crystal Chemistry and Physics of Metals and Alloys* (Wiley, New York, 1972), p. 76.
[6] Y. S. Jung, O. Kononenko, J. S. Kim, and W. K. Choi, J. Cryst. Growth **214**, 418 (2005).
[7] Y. S. Jung, O. Kononenko, N. Panin, and W. K. Choi, J. Appl. Phys. **99**, 013502 (2006).
[8] H. J. Ko, Y. F. Chen, S. K. Hong, H. Wenisch, T. Yao, and D. C. Look, Appl. Phys. Lett. **77**, 3761 (2000).
[9] K. Miyamoto, M. Sano, H. Kato, and T. Yao, Jpn. J. Appl. Phys., Part 2 **41**, L2103 (2002).
[10] D. Reynold, C. W. Litton, and T. C. Collins, Phys. Rev. **140**, A1726 (1965).
[11] B. K. Meyer, H. Alves, D. M. Hofman, W. Kriegseis, D. Forster, F. Bertram, J. Christen, A. Hoffman, M. Strsburg, M. Dworzak, U. Haboeck, and A. V. Rodina, Phys. Status Solidi B **241**, 231 (2004).
[12] E. F. Schubert, I. D. Goepfert, W. Grieshaber, and J. M. Redwing, Appl. Phys. Lett. **71**, 921 (1997).
[13] E. O. Kane, Phys. Rev. **131**, 79 (1963).
[14] T. Makino, Y. Segawa, S. Yoshida, A. Tsukazaki, A. Ohtomo, and M. Kawasaki, Appl. Phys. Lett. **85**, 759 (2004).
[15] J. D. Ye, S. L. Gu, S. M. Zhu, S. M. Liu, Y. D. Zheng, R. Zhang, and Y. Shi, Appl. Phys. Lett. **86**, 192111 (2005).
[16] D. C. Reynolds, D. C. Look, and B. Jogai, J. Appl. Phys. **88**, 5760 (2000).
[17] E. Hanamura, J. Phys. Soc. Jpn. **28**, 120 (1970).

All in-text references underlined in blue are linked to publications on ResearchGate, letting you access and read them immediately.
Downloaded 16 May 2011 to 143.248.111.110. Redistribution subject to AIP license or copyright; see http://jap.aip.org/about/rights_and_permissions